RSC Advances

A study of nanostructured ZnS polymorph by synchrotron X-ray diffraction and atomic pair distribution function

Journal:	*RSC Advances*
Manuscript ID	RA-ART-03-2016-005653.R1
Article Type:	Paper
Date Submitted by the Author:	14-Apr-2016
Complete List of Authors:	Gawai, U; Dr. Babasaheb Ambedkar Marathwada University, Department of Physics Khawal, H; Dr. Babasaheb Ambedkar Marathwada University, Department of Physics Bodke, Milind; Dr. Babasaheb Ambedkar Marathwada University, Physics Pandey, Krishan; Bhabha Atomic Research Centre, High Pressure & Synchrotron Radiation Physics Division Deshpande, Uday; UGC-DAE Consortium for Scientific Research, Lalla, N.; UGC-DAE Consortium for Scientific Research, Dole, Babasaheb; Dr. Babasaheb Ambedkar Marathwada University, Physics
Subject area & keyword:	Nanomaterials properties < Nanoscience

RSC Advances

PAPER

A study of nanostructured ZnS polymorph by synchrotron X-ray diffraction and atomic pair distribution function†

U. P. Gawai,[a] H. A. Khawal,[a] M. R. Bodke,[a] K. K. Pandye,[b] U. P. Deshpande,[c] N. P. Lalla,[c] and B. N. Dole*[a]

Received 00th January 20xx,
Accepted 00th January 20xx

DOI: 10.1039/x0xx00000x

www.rsc.org/advances

The atomic structure of polymorph Zn-S nanocube and nanowires has been studied using atomic pair distribution function (PDF) analysis and total synchrotron X-ray scattering data. PDF of sample S1 shows face centered cubic packing and sample S2 shows hexagonal closed packed structure. Phase transformations were observed with homogenous and nonhomogeneous treatment of temperature. Samples were synthesized by a hydrothermal method. PDF suggested that cation-cation (Zn^{+2}-Zn^{+2}) distance for S1 and S2 at 3.85 Å with coordination number ~1 and ~4 respectively. The core structure of cubic ZnS nanostructure with extensive stacking faults was confirmed by TEM. The diameters of the samples were extracted using PDF data which are in good agreement with the TEM results.The FE-SEM and TEM results that the sample S1 and S2 having nanocube and nanowires like structures respectively. The interatomic distance was calculated considering PDF analysis. The energy band gap of samples was estimated using UV-Vis spectra. It was observed that energy band gap goes on decreasing during structural transformation from cubic to wurtzite structure.

Introduction

Semiconducting nanomaterials have great attention for both applied as well as fundamental researchers. ZnS is an important II-VI group diluted magnetic semiconductor (DMS) material which has wide band gap of 3.77 eV for wurtzite[1] structure, and 3.72 eV for cubic[2] structure at 300 K with a large exciton binding energy (~40meV). ZnS has been used as a cardinal base materials for cathode ray tube (CRT) and field emission display (FED) Phosphors,[3-4] electroluminescent device, Light emitting diodes (LEDs),[5] Infrared (IR) window,[6]Field Effect Transistors (FETs)[7] and sensors.[8]

Most of the people are interested to investigate the different morphologies like nanoparticles,[9] nanorods,[10, 11] nanowires,[12, 13] nanoribbins,[14] and nanotube,[15] these have been synthesized by various techniques such as chemical method,[10] hydrothermal method,[16-20] thermal evaporation method,[21] pulse laser deposition,[22] electrochemical deposition,[23] molecular beam epitaxy (MBE),[24] microwave assisted technique,[25] chemical vapor deposition [26] etc.

Now-a-day synchrotron X-ray diffraction (SCXRD) with fast computing methods has been used for the determination of atomic scale structure of materials. SCXRD is also powerful tool to attain the structure of atoms with shorter length scales.[27] X-ray diffraction (XRD) used for the determination of crystal structure of nanocrystals, it acts as grating and produces a diffraction pattern of shows (Braggs peaks) crystal structure. Bragg peaks are arising due to translational symmetrywhich is present in the samples. However, the traditional XRD method breaks down when shorter wavelength of high energy X-raywas employed to study the crystal structure of materials. Recently rapid development in the nanoscience and nanotechnology has posed new challenges to study the atomic-scale structure using the XRD. Due to nanocrystalline nature of materials it does not always act as perfect grating hence XRD patterns show both Bragg peaks and diffuse component[28].

The pair distribution function (PDF) is one of the versatile method which can be applied to any materials. This method has numerous applications to analyze the structures of nanomaterials for determining crystal phase and unit-cell parameters and for quantifying various types of disorder or defects.[28-29] Also the PDF has one of the special approaches which are developed to analyze diffuse (non-Braggs type) XRD patterns. PDF can be applicable to the determination of the local structure, degree of disorder, stacking faults and diameters of the nanomaterials. It gives the probability of finding an atom at certain distance to another atom; which reveal the cation-cation and cation-anion and anion-anion bond lengths. PDF is the Fourier transform of normalization of total X-ray scattering. The PDF techniques, and total-scattering methods, allow both the Bragg and diffuse scattering to be analyzed together without bias, revealing the short and intermediate range order of the material regardless of the degree of disorder.[29-35] PDF is a local structural technique which demonstrates the quantitative structural information at the nanoscale from synchrotron X-ray[35], neutron,

[a] Advanced Materials Research Laboratory, Department of Physics, Dr. Babasaheb Ambedkar Marathwada University, Aurangabad-431 004, India. Email: drbndole.phy@gmail.com
[b] High Pressure & Synchrotron Radiation Physics Division, Bhabha Atomic Research Centre, Mumbai India.
[c] UGC DAE CSR, University Campus, Khandwa Road, Indore-452 001, India.

†Electronic Supplementary Information (ESI) available: Detailed information is given in ESI about XPS and EDAX and FTIR measurement. In ESI fig. 1 represent S1 XPS, fig. 2 gives S2 EDAX and fig. 3. Show FTIR spectra of samples S1 and S2.
See DOI: 10.1039/x0xx00000x

and electron diffraction[35] data. PDF is a potentially powerful technique due to modeling program.[36]

Herein we report the synchrotron X-ray diffraction method for details analysis of the atomic structure of polymorph of ZnS which was recorded at Beamline BL-11 of INDUS-II, RRCAT, Indore, India. The SCXRD data of S1 and S2 samples were analyzed using different computing program. Also we present detailed analysis of ZnS structures using PDF data. There are no reports available in literature on high energy X-ray atomic PDF analysis of polymorph ZnS nanomaterials. Masadeh et al.[30] and Yang et al.[36] reported that CdSe nanoparticles are best fitted by a mixture of crystalline structures intermediate between zinc blende and wurtzite structure. The same trend have been used for zinc blende and hexagonal structure of sample S1 and S2, which shows the intermediate structure between zinc blende and wurtzite structure and it is the grand success of this study. Using PDF data interatomic distances were evaluated considering total scattering structure function. TEM study candidly outlines sample S1 shows the stacking fault and S2 shows nanowires. Also a controllable synthesis of two phases of ZnS samples was discussed quantitively at low temperature 185 ^{0}C.

Experimental details

A hydrothermal method was used to synthesize polymorph of ZnS nanomaterials. In typical synthesis process 100 ml Teflon-lined stainless steel autoclave was used. All of the chemicals were of analytical grade and used without any further purification. The reaction was carried out as appropriate amounts of zinc nitrate (1 mmole), and thiourea (2 mmole) were dissolved in 75ml deionized (DI) water and ethylenediamine (1:1 ratio) solution. Then two solutions of same amount were prepared these solutions were stirred for 20 min. using magnetic stirrer at room temperature and these dispersed solutions were transferred in two autoclave separately. Then these autoclaves were sealed and kept S1 on hot plate and S2 in furnace at 185^{0}C temperature for 8 hours then allowed cooling naturally. Then obtained S1 and S2 product was centrifuged and washed for several time by ethanol and DI water and filtered. After this final product was dried in vacuum for 2 hours at 60 ^{0}C.

As synthesized samples were characterized using different characterization techniques. Synchrotron X-ray diffraction patterns were recorded with mode angle dispersive X-ray diffraction (ADXRD) from Beamline (BL-11) at INDUS-2, RRCAT Indore, India at room temperature and atmospheric pressure. The synchrotron X-rays diffraction patterns of nanowires were produced using wavelength of 0.378377 Å with the energy ~33 keV. Fourier transform infrared (FTIR) absorption spectrum was obtained with Bruker Vertex 70 spectrometer. UV-Vis absorption spectrum was taken on Perkin Elmer lambda-950 UV-Vis spectrophotometer.Electron Spectroscopy for Chemical Analysis (ESCA) was produced using X-ray photon energy of Al Kα: 1486.61 eV, 13 KV, and 300 W from Phoibos analyzer. Field emission scanning electron microscopy (FE-SEM) image and energy dispersive spectra (EDS) were collected from JEOL JSM-6360 SEM. Transmission electron microscopy (TEM) measurement was undertaken at accelerating voltage 200 kV and selected-area electron diffraction (SAED) patterns were carried out with a Tecnai G^2 20 at an acceleration voltage at 200 kV.

Results and discussion

Synchrotron X-ray Diffraction study

The Synchrotron X-ray Diffraction (SCXRD) patterns of samples S1 and S2 are shown in fig. 1. The SCXRD measurements have been achieved by monochromatic white synchrotron beam using Si (111) channel cut monochromator. All samples were sealed to kapton foils for further measurements. The 2D images were recorded at 2D image plate camera MAR 345 with imaging plate 50x30 µm using compound refractive lens. These 2D images were calibrated using silicon standard. The obtained scattering signal from the samples was measured independently and subtracted from background in the data reduction. Then collected 2D diffraction images were combined and subjected to geometric correction, integrated and converted to intensity verses 2θ using the FIT2D[50] program. ZnS materials exhibit medium range order atomic order which is expected from ADXRD[16] patterns of crystalline ZnS show well defined Braggs peaks at Q=10.2 Å^{-1}. SCXRD revealed high resolution diffraction for structural refinement. The entire diffraction peak of S1 sample can be readily indexed as sphalerite structure while S2 indexed as wurtzite structure. There are no secondary phases observed in the prepared samples. The SCXRD results are very close to the standard values card no. (JCPDS-80-0007 space group, $P6_3mc$

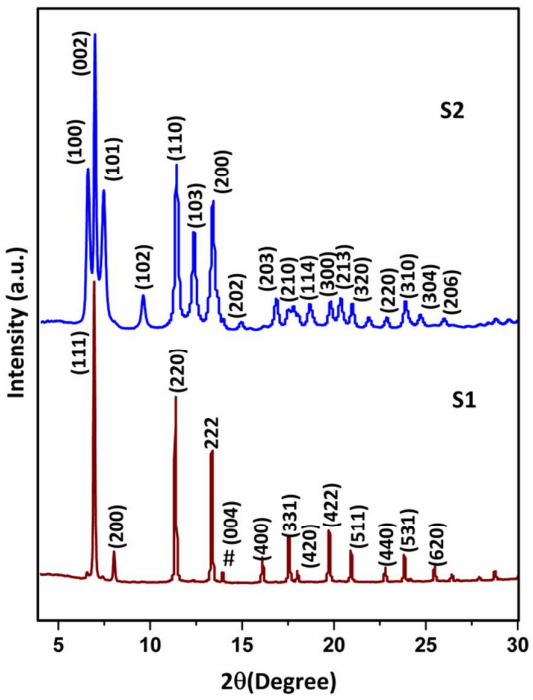

Fig. 1 SCXRD patterns of samples S1 and S2 which show the cubic and hexagonal structures.In the S1 sample a peak observed at (004) indicates that the wurtzite phase of ZnS.

(186)) with a = 3.777 Å, c = 6.188 Å for wurtzite and JCPDS-80-0020space group $F\bar{4}3m$ (216) with a = 5.4145 Å cubic structures. Thus for S2 full width at half maxima (FWHM) of the (002) peak is stronger and narrowest among all peaks, which indicates that nanowires are grown in the (002) direction, it is further evidenced by through TEM

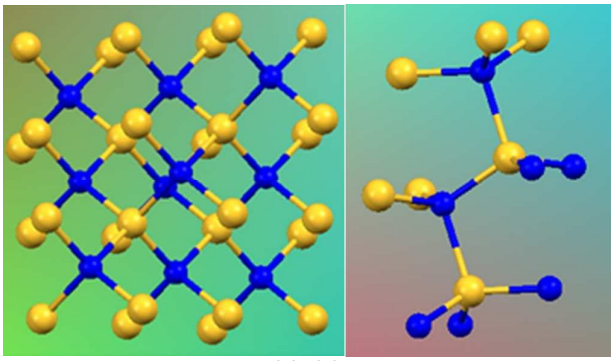

(a) (b)

Fig. 2 Optimized geometries of the **(a)** spheralite (Zinc blende) structure space group $F\bar{4}3m$ of S1 and **(b)** wurtzite structure space group $P6_3mc$ of S2 as generated from Rietveld refinement.Yellow coloured balls represent Zn atoms and blue coloured balls represent S atoms.

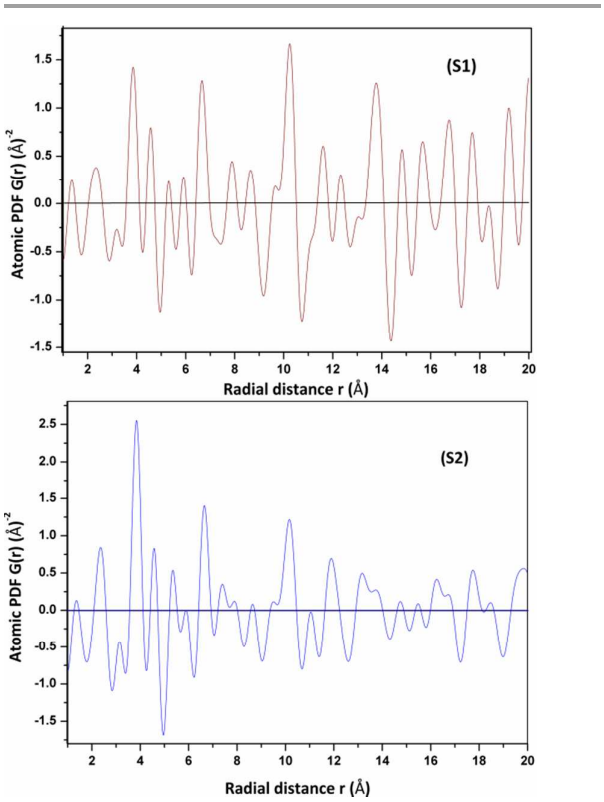

Fig. 3 The experimental Pair distribution function (PDF) G(r) of ZnS samples S1 and S2. Here S1 and S2 corresponding to spheralite and wurtzite structures respectively.

analysis. In the S1 sample (111) diffraction peak is stronger than others. Lattice parameters were calculated using SCXRD data and their values are tabulated in table 1. However no extra peaks of alloy or oxide phases were detected as the cubic to wurtzite phase transformations.

Atomic pair distribution function Analysis

In order to investigate the core structure of polymorph ZnS samplesthe SCXRD and PDF technique were combined. In the same materials with different morphology and structure show drastic changes in SCXRD and PDF. SCXRD was employed to obtain the PDF from AD/ED-XRD BL-11 beamline at Raja Ramanna Center for Advanced Technology (RRCAT), Indore. For the purpose of PDF, data were corrected and normalized using the program PDFGetX3-1.1.[38] Pair distribution function G(r) was plotted which reveals the probability of finding certain distance 'r' between atoms.The atomic PDF is formally defined as,

$$G(r) = 4\pi r[\rho(r) - \rho_0] \quad (1)$$

Where ρ(r) is the atomic pair density, ρ_0 is the average atomic number density and r is the radial distance.[39,41]

The total scattering technique outlines Braggs peak with position and intensity gives structure and diffuse scattering with deviation gives perfect lattice. The PDF G(r) is a one dimensional function which oscillates around zero and indicates peak position at distance separation pairs of an atom.The peaks position of the PDF corresponded to the distribution of distances in the material. The negative valley in the PDF corresponding to the real-space vector not having atoms at either of their ends, owing to this reason PDF resembles Patterson function therefore it is widely applicable for X-ray crystallography study[29]. Fourier analysis of the total scattering is known as atomic PDF analysis, means PDF is the Fourier transform of the scattering intensity. PDF was obtained using the total scattering structure function S(Q) considering Fourier transformation is given in equation[40] (2). The PDF G(r) is obtained by a sine Fourier transformation of the reciprocal space total scattering structure S(Q) function of diffraction data.

Where Q is the magnitude of the wave vector and is derived from Q

$$G(r) = \frac{2}{\pi}\int_{Q=0}^{Q_{max}} F(Q)\, sin(Qr) dQ \quad (2)$$

$$G(r) = \frac{2}{\pi}\int_{Q=0}^{Q_{max}} Q[S(Q) - 1]\ sin(Qr)\, dQ \quad (3)$$

= 4π sin (θ)/λ, λ is the wavelength of X-rays, θ is the half scattering angle.[39,40] The Faber-Ziman type total structural function S(Q) was related to the diffraction patterns as well as$I^{coh}(Q)$ and the relation of S(Q) is given below,

$$S(Q) = 1 + \left[I^{coh}(Q) - \sum c_i |f_i(Q)|^2\right] / \left|\sum c_i f_i(Q)\right|^2 \quad (4)$$

Where $I^{coh}(Q)$ is the coherent scattering intensity per atom in electron units and c_i is the atomic concentration, $f_i(Q)$ is X-ray scattering factor for atomic species type i[39]. Here we report $Q_{max} = 10.2$ Å^{-1} at ~33 KeV is optimized to avoid large terminal effect and reduce signal to noise ratio. The G(r) gives probability of finding a neighbor atom at distance r. From the PDF patterns spheralite and hexagonal structures were confirmed with space

group $F\bar{4}3m$ and P6$_3$mc respectively. Sulfide semiconductor materials may show two well-known structures as zinc blende and wurtzite structure with identical shared tetrahedral bonding fordifferent stacking sequences. The close-packed stacking sequences for wurtzite structure is ABABAB…along (001) orientation whereas for zinc blende structure the close-packed stacking sequence is ABCABC…along (111) orientation. Here we tried to synthesized and model/refine these two structure with constrain isotropic ADPs for spheralite and anisotropic ADPs for wurtzite structure. The sharp and well resolved peaks in PDF suggest high symmetry and a well-defined local structure of ZnS samples. The PDFs are shown in fig. 3 which gives the interatomic distances from peaks values. The first nearest neighbor distance for S1 and S2 are at r = 2.3478 Å and r=2.335 Årespectively from covalently bounded Zn^{2+}-S^{-2} pair. The second strong and intense peak is of metal-metal bonding distance at 3.834 and 3.833 Å, which representing Zn^{2+}-Zn^{2+} for S1 and S2 respectively. It is visualized that the finite particle size or diameter is evident in a falloff in the intensity of structural feature with increasing radial distance. The ZnS average particle size or diameter has been extracted from PDF. It was observed that S1 is having average diameter 22.9 nm and S2 has 15.6nm.

Quantitative structural information can be extracted from refinement of PDF by comprising the observed PDF and calculated PDF from models. The PDFgui computer program[51] was used to fit and simulate structural model to the experimental PDF shown in fig. 4 and 5. In fig. 4(a) S1 we treated as zinc blende/ spheralite structure with spheralite structure model fig. 4(b) S2 reflects wurtzite structure over wurtzite modeling using isotropic ADPs. These two structures gives best fit for S1 and S2 structures as experimental and calculated PDF from refinement, it is agreement with residual function. Whereas in fig. 5 (a) we model cubic structure with wurtzite and in fig. 5(b) wurtzite with spheralite

$$R_w = \sqrt{\frac{\sum_{i=1}^{N} \omega(r_i)[G_{obs}(r_i) - G_{calc}(r_i)]^2}{\sum_{i=1}^{N} \omega(r_i) G_{obs}^2(r_i)}} \quad (5)$$

structure. In the fig. 5 we observed some peaks matches at certain extent of 'r'. It means that there is possibility of multi-phase at the

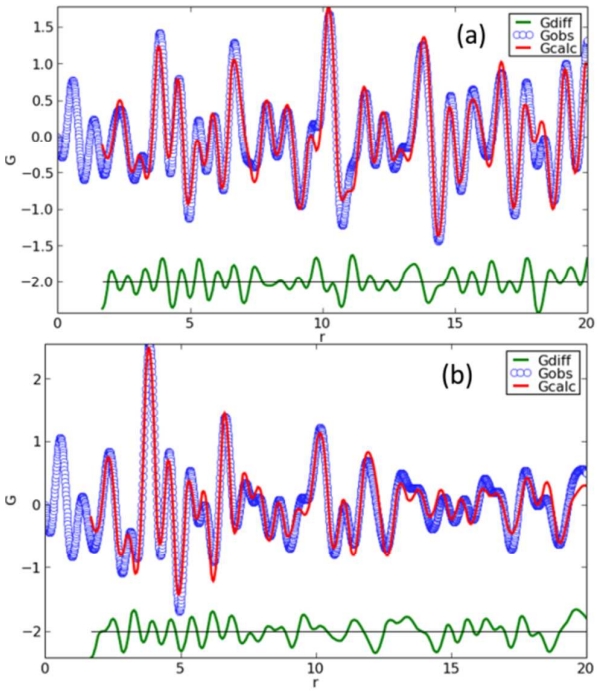

Fig. 4 The refined structural PDF of **(a)** spheralite S1 **(b)** wurtzite S2 structure with G_{obs} means experimental PDF.

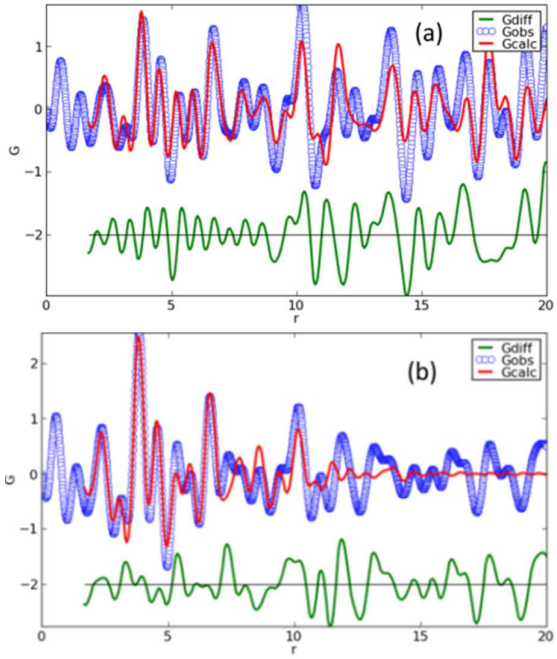

Fig. 5 The experimental PDF G(r) and calculated refined PDF with difference curve offset below. PDF data fitted using S1 **(a)** wurtzite structure model with space group $P6_3mc$ and S2 **(b)** zinc blende structure model with space group $F\bar{4}\,3m$in both models isotropic ADPs used.

Table 1 The refined parameterobtained from PDF analysis of ZnS samples.

Structural parameters		S1	S2
Zinc-Blende	a (Å)	5.4222	5.4223
	Unit cell volume	159.416	159.441
	Zn U_{11}=U_{22}=U_{33}	0.011542	0.000798
	S U_{11}=U_{22}=U_{33}	0.00466862	0.036331
	Q_{damp}	0.0420	0.1770
	Zn-S	2.3478	2.34795
	Zn-Zn	3.83409	3.83418
	R_w	0.250	0.551
	Diameter	22.9nm	4.8 nm
Hexagonal	a(Å)	3.8327	3.83302
	c(Å)	5.8474	6.26669
	Unit cell volume	74.3899	79.7357
	Zn U_{11}=U_{22}	0.000278	0.006452
	U_{33}	0.2148	0.008578
	S U_{11}=U_{22}	0.000798	0.001206
	U_{33}	0.002932	0.13555
	S Z_{frac}	0.387043	0.38084
	Q_{damp}	0.04319	0.07528
	Zn-S	2.26322	2.335
	Zn-Zn	3.60989	3.83314
	R_w	0.6181	0.2820
	Diameter	∞	15.6nm

same structures. The values of refined parameters are summarized in table 1 of their respective fit which manifested in fig. 4 and 5. Where G_{obs} is the PDF extracted from the diffraction data,G_{cal} is the PDF calculated from the model and $\omega(r_i)$ is weight. The structural parameters of the model were unit cell parameter,anisotropic atomic displacements (ADPs) for the Zn and S atom. A generated simulated PDF from calculated data which is in excellent agreement with the experimental data. The resulting very low residual signal intensity across the fitting range is for samples S1 R_w=0.2 and S2 R_w=0.38 (fitting range = 1.7 to 20Å).

Optical property: Diffuse reflectance spectra

The UV-Vis absorption spectra of semiconductor nanoparticles depend on their size whereas absorption minimum increases with the particle size[42]. UV-Vis diffuse reflectance spectra (DRS) were

$$\alpha h\upsilon = A\left(h\upsilon - E_g\right)^{\frac{1}{2}} \qquad)$$

recorded of samples considering $BaSO_4$ as background with wavelength 200 to 850 nm. The UV-Visible absorption spectra of S1 and S2 are shown in fig.6(a). The energy band gap was calculated using Tauc equation[43] (6).

Where α is the absorption coefficient, hν is the photon energy, A is a band edge sharpness constant, E_g is the energy band gap of the

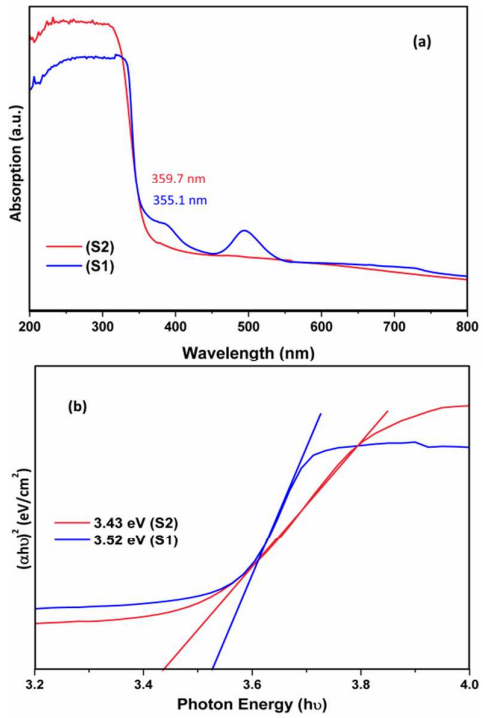

Fig. 6 UV-Vis diffuse reflectance spectra **(a)** shows absorption spectra of samples S1 and S2 and **(b)** shows its corresponding Tauc plot for the evaluation of energy band gap.

sample. From the Tauc plot fig. 6(b) the energy band gap is found to be 3.52 and 3.43 eV for S1 and S2 respectively. It is observed that the band gap of spheralite S1 is higher thanwurtzite S2 structure which may be due to staking faults present in the sample S1.

XPS study

The XPS was employed for the confirmation of chemical composition of the samples. The XPS analysis of sample S2 was scanned in the range of 0–1400eV and its survey spectrumis shown ESI† fig.1(a) (Detailed information about XPS and EDAXis given in ESI†). It shows that Zn and S were present in the synthesized samples. No contaminant species were observed within the sensitivity range of the technique. The corrected peak position of binding energy observed for $Zn2p_{3/2}$ and $Zn2p_{1/2}$ are at 1020.63 and 1043.81 eV respectively.[46-50] In fig. 7(a), the spin–orbit splitting of $Zn2p_{3/2}$ and $Zn2p_{1/2}$ is found at 23.18 eV for Zn^{2+} state on the basis of peak positions of Zn2p. From S2p it is observed with overlapping spin-orbit doublets.The binding energy of S2p centered at 160.69 eV which is characteristics value of metal sulfide (S^{2-}) species.[47-50]From the fig. 7(b) Gaussian fit corresponding to $S2p_{3/2}$ and $S2p_{1/2}$ shows binding energy at 160.57eV and 161.71eV respectively with splitting 1.14eV. The appearance of all the binding energy values for Zn 2p and S 2p are in accordance with previously reported position for ZnS compound. The binding energy values for the Zn3p Zn3d and S2s are given in ESI†. With further detailed examinations, the

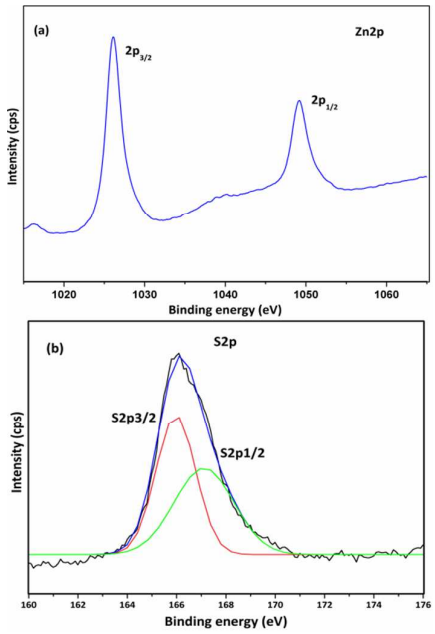

Fig. 7XPS spectra of **(a)** Zn2p and **(b)** S2p of S2 sample.

compositions of ZnS from XPS as well as EDAX are consistent with stoichiometric Zn to S free of other impurities such as carbon. From FTIR ESI† fig. 3, it can be further confirmed the chemical species present in the samples (detailed analysis is given in ESI†).

Morphological investigation

The transmission electron microscopy (TEM) and field emission scanning electron microscopy (FE-SEM) were used to examine the morphology of the samples S1 and S2. TEM was employed to investigate structural morphology of ZnS samples. To evaluate the distribution of spheralite to wurtzite structure of samples S1 and to identify the microstructure, coarseness and stacking faults present in S1 was evidently examined via TEM and refine PDF (fig. 5a) with R_w=0.618. Huang et al.[45] reported that the stacking faults was

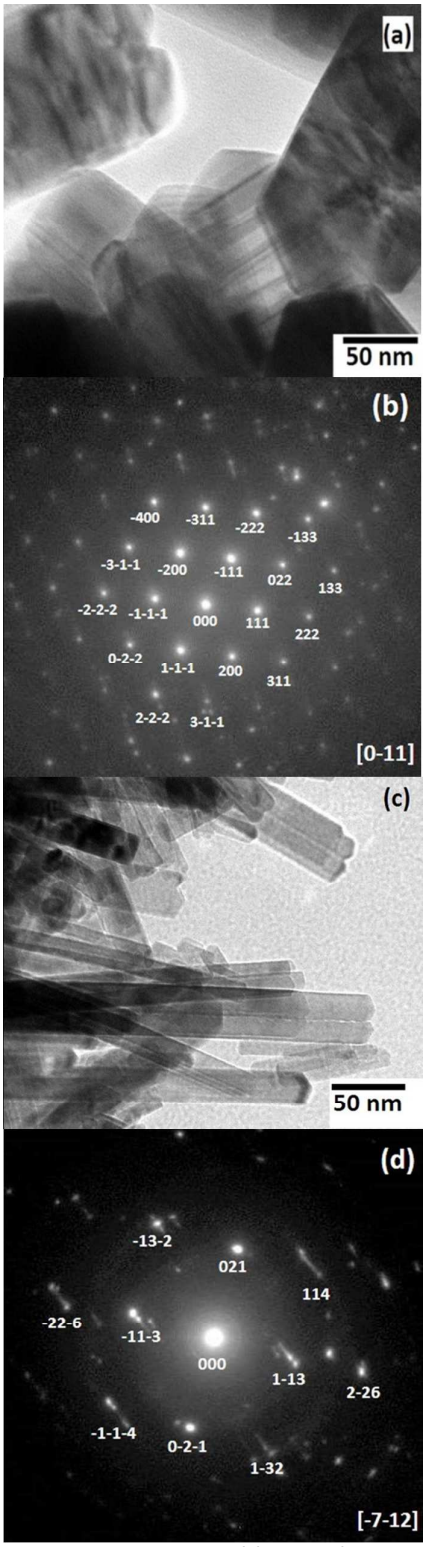

Fig. 8 TEM image of samples **(a) S1** and (**c) S2** with SAED patterns**(b)** and **(d)**respectively.

observed at 225 ^{0}C, but in our case stacking faults were observed at temperature ~185^{0}C (inhomogeneous heating) for 8 h with autoclavewas placed on hotplate (inhomogeneous heating). TEM of sample S1 and S2 are shown in fig. 8 (a) and 8(c). TEM micrograph shows that extremely uniform diameter nanowires structure were observed in sample S2 whereas in sample S1 stacking faults indicating small dislocation were clearly observed. The average diameter for S2 is found to be 12 nm and length may be tens of micrometers. Also for S1 the average crystallite size is found to be 30 nm. The selected area electron diffraction (SAED) pattern of S2 also shows that the concentric rings which reflect hexagonal structure. TEM micrograph of S1 and S2 of ZnS samples shown in fig. 8 (a, c) and its corresponding SAED patterns are depicted in the fig. 8(b, d) respectively. The spheralite structure which corresponding SAED patterns in the fig. 8(b) reflects that the single crystalline nature of S1 sample, whereas SAED patterns in fig 8(d) reveals that polycrystalline nature of S2 sample. The SAED patterns can be indexed as that recorded along [0-11] and [-7-12] zone axis

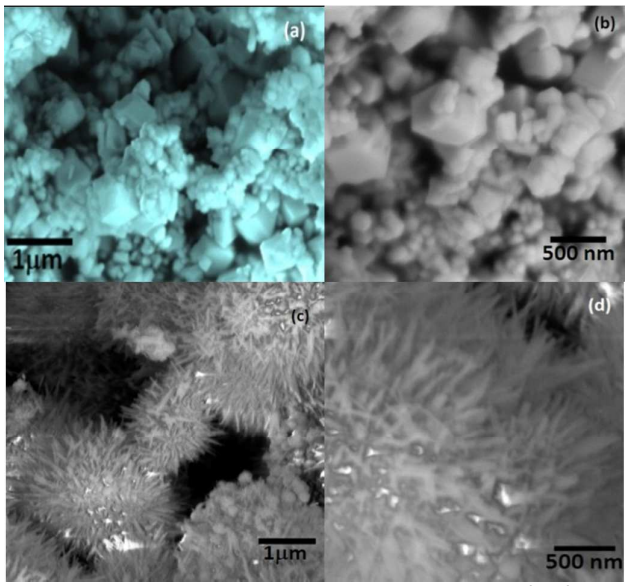

Fig. 9 The different magnified FE-SEM images of samples S1 **(a, b)** and S2 **(c, d)** respectively.

of samples S1 and S2 respectively. Fig. 9 shows the FE-SEM images of S1 and S2. In FE-SEM images fig. 9(a, b) some 3D nanocubes and tiny particles were observed for S1, while in fig. 9(c, d) nanowires like structures were observed for sample S2.

Conclusions

Polymorph of ZnS nanocube and nanowires were successfully synthesized by a hydrothermal method at low temperature 185^{0}C in the presence of ethylenediamine as the soft template. The synchrotron X-ray diffraction was employed for PDF analysis. The PDF was utilized to address the atomic scale structure of ZnS samples S1 and S2. Total X-ray diffraction coupled to PDF data analysis which allows to determine the presence of nanoscale inhomogeneity in the structure. The synthesized sample S1 and S2 of ZnS have spheralite and hexagonal (wurtzite) structures respectively. The energy band gap of ZnS samples shows more red shift as compared to the bulk ZnS band gap. The chemical species of samples S1 and S2 are confirmed from FTIR spectra. It has been observed from FE-SEM and TEM image analysis that the

morphology of samples S1, S2 are nanocubes and nanowires like structures. The SAED patterns of S1 and S2 indicated single crystalline and polycrystalline nature of ZnS. The combination of synchrotron X-ray diffraction and atomic PDF has the potential tool for the standardizations of atomic scale structure of nanomaterials.

Acknowledgements

The authors are grateful to UGC-DAE CSR, Indore for financial assistance through Project No.CSR-1/CSR-66/2012-13/270, Dr. T. Shripathi, UGC-DAE CSR, Indore and Prof. S. S. Shah for his encouragement.

References

1 H. C. Ong and R. P. H. Change,*Appl.Phys.Lett.,*2001, **79,** 3612.
2 T. K. Tran, W. Park, W. Tong, M. M. Kyi, B. K. Wagner and C. J. Summer, *J. Appl. Phys*.1997,**81,** 2803.
3 Z. Zhong, D. Wang, Y. Cui, M. W. Bockrath, C. M. Lieber, *Science*, 2003, **302**, 1377.
4 Z. Zhong, F. Qian, D. Wang, C. M. Lieber, *Nanolett.* 2003, **3,** 343.
5 P. Calandra, m. Goffredi and V. T. Liveri, *Colloids Surf. A,*1999, **160,** 9.
6 Y. Cui, Q. Wei, H. Park, C. M. Lieber, *Science*, 2001,**293,** 1289.
7 Z. G. Chen, L. Cheng, H. V. Xu, J. Z. Liu, J. Zou, T. Sekiguchi, G. Q. M. Lu and H. M. Cheng, *Adv. Mater*, 2010, **22,** 2376.
8 M. J. Ruedas-Rama, A. Orte, E. A. H. Hall, J. M. Alvarez-Pez and E. M. Telavera, *Chem. Comman.,*2011, **47,** 2898.
9 M. R. Bodke, H. A. Khawal, U. P. Gawai, B. N. Dole, *open AccessLibrary Journal,* 2015, **2**:e1549.
10 S. A. Acharya, N. Maheshwari, L. Tatikondewar, A. Kshirsagar, S. K. Kulkarni, *Cryst. Growth Des.,* 2013, **13,** 1369-1379.
11 M. V. Limaye, S. Gokhale, S. A. Acharya and S. K. Kulkarni, *Nanaotechnology, 2008,***19,** 415602.
12 P. Jiang, J. Jie, Y. Yu, Z. Wang, C. Xie, X. Zhang, C. Wu, L. Wang, Z. Zhu and L. Luo, *J. Mater. Chem.,*2012, **22**, 6856.
13 C. Y. Wu, J. S. Jie, L. Wang, Y. Q. Yu, Q. Peng, X. W. Zhang, J. J.Cai, H. Guo, D. Wu and Y. Jiang, *Nanotechnology*, 2010, **21,** 505203.
14 S. Kar, S. Chaudhuri*, J. Phys. Chem. B*, 2005, **109**, 3298 3302.
15 S. A. Acharya, S. S. Bhoga and k. Singh, *Integrated Ferroelectrics,*2010, **116,** 16-22.
16 U. P. Gawai, H. A. Khawal, T. Shripathi and B. N. Dole, *CrystEngComm,* 2016, **18,** 1439-1445.
17 S. K. Pahari, A. Sinhamahapatra, N. Sutradhar, H. C. Bajaj and A. B. Panda, *Chem. Commu*, 2012, **48**, 850-852.
18 J. Cao, D. Han, B. Wang, L. Fan, H. Fu, M. Wei, B. Feng, X. Liu, J. Yang*, Journal of Solid State Chemistry,* 2013, **200,** 317-322.
19 M. Wei, J. Yang, Y. Yan, J. Cao, Q. Zuo, H. Fu, B. Wang, L. Fan, *super lattices and microstructures*, 2013, **54**, 181-187.
20 J. Cao, L. Fan, J. Yang, Y. Yan, M. Wei, L. Yang, B. Feng, B. Han, B. Wang, H. Fu, *Super lattice and microstructure*, 2013,**57,** 58-65.
21 M. Lu, L. Chen, W. Mai, and Z. L. Wang, *App. Phys. Lett*., 2008,**93,** 242503.
22 X. Xu, G. Fei, W. Yu, X. Wang, L. Chen and L. Zhang, *Nanotechnology,*2006, **17,** 426-429.
23 R. Chem, D. Li, B. Liu, Z. Peng, G. G. Gurzadyan, Q. Xiong and H. Sum*, Nano Lett.,* 2005, **10**, 4956-4961.
24 K. Inchino, H. Yoshida, T. Kawai, H. Matsumoto, H. Kobayashi, *Journal of the Korean Physical Society*, 2008,**53** (5), 2939-2942.
25 M. Navaneethan, J. Archana, K. D. Nisha, S. Ponnusamy, M. Arivanandhan, Y. Hayakawa, C. Muthamizhelven, *Material Letters*, 2012, **66**, 276-279.
26 M. Huang, Y. Cheng, K. Pan, C. Chang, F. S. Shieu, H. C. Shih, *Applied Surface Science*, 2012, **261,** 665-670.
27 V. Petkov, *materialstoday,*2008,**11,**28-38.
28 V. Petkov, S. J. L. Billinge, P. Larson, S. D. Mahanti, T. Vogt, K. K. Rangan, and M. G. Kanatzidis, *Phys. Rev. B, 2002,***65**, 092105.
29 V. Petkov, P. Y. Zavalij, S. Lutta, M. S. Whittingham, V. Parvanov ,andS. Shastri, *Phys. Rev. B*, 2004, **69**, 085410.
30 A. S. Masedeh, E. S. Bozin, C. L. Farrow, G. Paglia, P. Juhas, S. J. L. Billinge, A. Karkamkar, and M. G. Kanatzidis, *Phys. Rev. B*, 2007, **76**, 115413.
31 W. Li, R. Harrington, Y. Tang, J. D. Kubicki, M. Aryanpour, R. J. Reeder, J. B. Parise and B. L. Phillips, *Environ. Sci. Technol*., 2011, **45,** 9687-9692.
32 C. Tyrsted, K. M. O. Jensen, E. D. Bojesen, N. Lock, M. Christensen, S. J. L. Billinge and B. B. Iversen, *Angew. Chem. Int. Ed.,*2012, **51**, 9030-9033.
33 M. Gateshki, M. Niederberger, A. S. Deshpande, Y. Ren and V. Petkov*, J. Phys.,:Condens. Matter,*2007, **19**, 156205.
34 M. Abeykoon, C. D. Malliakas, P. Juhas, E. S. Bozin, M. G. Kanatzidis and S. J. L. Billinge, *ZeitschriftfürKristallographie Crystalline Materials* 2012, **227**, 248-256.
35 V. V. T. Doan-Nguyen, S. A. J. Kimber, D. Pontoni, D. Reifsnyder Hickey, B. T. Diroll, X. Yang, M. Miglierini, C. B. Murray and S. J. L. Billinge, *ACS Nano,*2014,**8(6),** 6163-6170.
36 X. Yang, A. S. Masadeh, J. R. McBride, E. S. Bozin, S. J. Rosenthal and S. J. L. Billinge, *Phys. Chem. Chem. Phys.,* 2013, **15**, 8480.
37 Q. Lia and C. Wang, *Appl. Phys. Lett.,*2003, **83**, 359.
38 Y. Jiang, X. M. Meng, J. Liu, z. Y. Xie, C. S. Lee and S. T. Lee, *Adv. Mater. J. Phys. Chem. C.,*2010, **114,** 21366.
39 P. Juhas, T. Davis, C. L. Farrow and S. J. L. Billinge, *J. Appl. Cryst*. 2013, **46,** 560–566.
40 S. L. J. Billiange, M. G. Kanatzidis, *Chem. Commun.*2004, 749-760.
41 T. Egami, S. J. L. Billinge, *Underneath the Bragg peaks: structure analysis of complex materials, PargamonPress, Elsevier Oxford England*2003.
42 P. Calandra, M. Goffredi, V. L. Turco, *Coll. Surf. A,* 1999, **160,** 9-13.
43 J. Tauc, R. Grigorovici and A. Vancu, *Phys. Status Solidi,*1966, **15**, 627.
44 S. B. Qadri, E. F. Skelton, D. Hsu, A. D. Dinsmore, J. Yang, H. F. Gray, and B. R. Ratna*Physical Review B,*1999, **44,** 153.
45 F. Huang and J. F. Banfield, *J. Am. Chem. Sco.,* 2005, **127,** 4523-4529.
46 A. P. Hammersley, S. O. Svenson, M. Hanfland and D. Hauserman, High Pressure Res., 1996, **14**, 235–248.
47 J. Yang, H. Liu, W.N. Martens, R.L. Frost, *J. Phys. Chem. C*, 2010, **114,** 111.
48 D. Ban, F. Yang. R. Fang, S. Xu, P. Xu, *J. Electron Spectrosc. Relat. Phenom.*,1996, **80**, 197.
49 C. J. Powell, *J. Electron Spectrosc. Relat. Phenom.,*2012, **185,** 1.
50 G. Wang, B. H., Z. Li, Z. Lou, Z. Wang, Y. Dai and M-H Whangbo, *Scientific Reports,* 2015, **5,** 8544.
51 C. L. Farrow, P. Juhas, J. W. Liu, D. Bryndin, E. S. Bozin, J. Bloch, Th. Proffen and S. J. L. Billinge, *J. Phys.: Condens. Matter,*2007, **19**, 335219.

PCCP

GRAPHICAL ABSRACT

A study of nanostructured ZnS polymorph by synchrotron X-ray diffraction and atomic pair distribution function†

U. P. Gawai,[a] H. A. Khawal,[a] M. R. Bodke,[a] K. K. Pandye,[b] U. P. Deshpande,[c] N. P. Lalla,[c] and B. N. Dole*[a]

Received 00th January 20xx,
Accepted 00th January 20xx

DOI: 10.1039/x0xx00000x

www.rsc.org/

The combination of synchrotron X-ray diffraction and atomic PDF is the potential tool for the standardizations of atomic scale structure of nanomaterials. This articles discribe the essential approch and and potential of polymorph of nanocube S1 and nanowires S2 of ZnS samples.

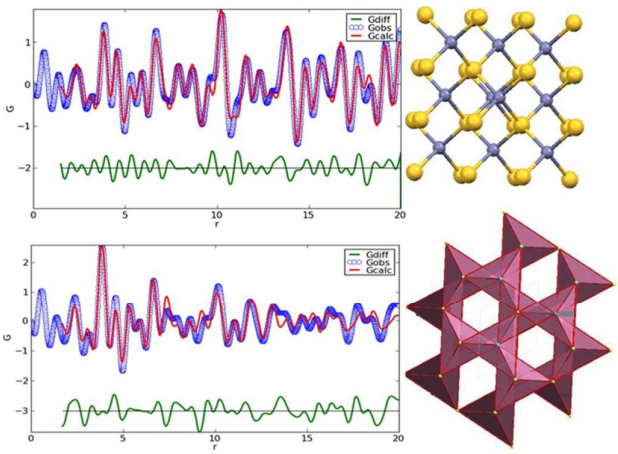

[a] Advanced Materials Research Laboratory, Department of Physics, Dr. Babasaheb Ambedkar Marathwada University, Aurangabad-431 004, India. Email: drbndole.phy@gmail.com
[b] High Pressure & Synchrotron Radiation Physics Division, Bhabha Atomic Research Centre, Mumbai India.
[c] UGC DAE CSR, University Campus, Khandwa Road, Indore-452 001, India.

†Electronic Supplementary Information (ESI) available: Details information is given in ESI about XPS and EDAX measurement.
See DOI: 10.1039/x0xx00000x